

Lawrence Berkeley National Laboratory

Recent Work

Title

GENERALIZED PAIRING IN LIGHT NUCLEI II: SOLUTION OF HFB EQUATIONS WITH REALISTIC FORCES AND COMPARISON OF DIFFERENT APPROXIMATIONS

Permalink

<https://escholarship.org/uc/item/15v2q52d>

Authors

Goodman, A.L.

Struble, G.L.

Bar-Touv, J.

et al.

Publication Date

1970

GENERALIZED PAIRING IN LIGHT NUCLEI II:
SOLUTION OF HFB EQUATIONS WITH REALISTIC
FORCES AND COMPARISON OF
DIFFERENT APPROXIMATIONS

RECEIVED
LAWRENCE
RADIATION LABORATORY

FEB 17 1970

LIBRARY AND
DOCUMENTS SECTION

A. L. Goodman, G. L. Struble,
J. Bar-Touv and A. Goswami

January 1970

AEC Contract No. W-7405-eng-48

TWO-WEEK LOAN COPY

*This is a Library Circulating Copy
which may be borrowed for two weeks.
For a personal retention copy, call
Tech. Info. Division, Ext. 5545*

LAWRENCE RADIATION LABORATORY
UNIVERSITY of CALIFORNIA BERKELEY

DISCLAIMER

This document was prepared as an account of work sponsored by the United States Government. While this document is believed to contain correct information, neither the United States Government nor any agency thereof, nor the Regents of the University of California, nor any of their employees, makes any warranty, express or implied, or assumes any legal responsibility for the accuracy, completeness, or usefulness of any information, apparatus, product, or process disclosed, or represents that its use would not infringe privately owned rights. Reference herein to any specific commercial product, process, or service by its trade name, trademark, manufacturer, or otherwise, does not necessarily constitute or imply its endorsement, recommendation, or favoring by the United States Government or any agency thereof, or the Regents of the University of California. The views and opinions of authors expressed herein do not necessarily state or reflect those of the United States Government or any agency thereof or the Regents of the University of California.

GENERALIZED PAIRING IN LIGHT NUCLEI II: SOLUTION OF HFB EQUATIONS WITH
REALISTIC FORCES AND COMPARISON OF DIFFERENT APPROXIMATIONS*

A. L. Goodman

Lawrence Radiation Laboratory, University of California
Berkeley, California 94720

and

G. L. Struble

Lawrence Radiation Laboratory and Department of Chemistry
University of California, Berkeley, California 94720

and

J. Bar-Touv

Lawrence Radiation Laboratory, University of California
Berkeley, California 94720

and

Ohio State University
Columbus, Ohio 43210

and

A. Goswami

University of Oregon
Eugene, Oregon 97403

ABSTRACT

The HFB equations with generalized isospin pairing are numerically solved without any approximations, except imposing certain self-consistent symmetries. Realistic forces are used to make definite conclusions concerning the shapes of nuclei and the existence of isospin pairing. Comparison with previous approximations shows that in the s-d shell the HFB equations may not be quantitatively approximated by HF + BCS, HB - BCS, or by iterating between HF and BCS. Isospin pairing restores axial symmetry to ^{24}Mg and ^{32}S and offers an explanation for the existence of low-lying vibrational states in ^{36}Ar .

I. INTRODUCTION

Nuclei in the first half of the s-d shell exhibit rotational features such as energy level spacings obeying an $I(I+1)$ law and enhanced electromagnetic transition probabilities between states within a rotational band. A very useful technique for calculating the wavefunctions of such states involves the construction of an intrinsic state and the subsequent projection of angular momentum using the Hill-Wheeler integral¹ or various approximations based on the adiabatic nature of the rotational motion.² Intrinsic states have been calculated using deformed potential models³ and more recently they have been calculated using Hartree-Fock (HF) theory. For a review of HF calculations in the s-d shell see Refs. 4 and 5.

The HF description fails for the $N = Z$ even-even nuclei beyond ^{20}Ne . These failures have been discussed in detail in a previous publication⁶ hereafter referred to as I. However to summarize the most important points of this discussion we note (1) there are several experimental investigations which strongly indicate that the intrinsic shape of ^{24}Mg is prolate and axial while HF unambiguously predicts the shape to be triaxial, (2) for ^{28}Si HF predicts both a low lying oblate and an orthogonal low lying prolate intrinsic state which is in contradiction to the experimental spectrum, (3) for ^{32}S HF predicts a triaxial shape⁷ with $\beta_2 = 0$ again in contradiction to the experimental spectrum, and (4) experiments suggest that ^{36}Ar can be interpreted phenomenologically as a vibrator while HF predicts a well deformed oblate intrinsic state giving low energy rotational levels. If we are to adopt the concept of an intrinsic state then a more complicated one must be used.

In I we pointed out that the Hartree-Fock-Bogoliubov method (HFB) might be useful for describing the intrinsic states in the s-d shell. Recently such

calculations have been carried out by two groups^{8,9} who both conclude that for $N = Z$ even-even nuclei the usual $J = 0$ pairing does not occur. As clearly pointed out in Ref. 9 and in I this result can not be taken to mean that HFB will not produce new intrinsic states since these authors have omitted neutron-proton correlations which have been shown to be important for $N = Z$ nuclei.¹⁰ In (I) we solved the HFB equations including neutron-proton correlations using an approximation similar to that employed by Kumar and Baranger.¹¹ In this paper we solve the HFB equations exactly and make a careful examination of approximations most usually employed in their solution and we also comment on the relevance of pairing in the intrinsic states of the $N = Z$ even-even nuclei in the s-d shell. We will use realistic interactions in this paper in order to make our conclusions about the existence of neutron-proton pairing and the shapes of these nuclei in a parameter free fashion. In Sec. II we briefly develop the formulation of HFB and discuss in some length the concept of self-consistent symmetry in HFB and the importance of the particular phases that we introduce. We also comment on the various approximations to HFB that have been used in discussing pairing. In Sec. III we describe our calculations, attempt to justify the solutions, and discuss the effects of truncation and the imposition of self-consistent symmetries. In Sec. IV we give the results of our calculations discussing the validity of previous approximations, while in Sec. V we discuss the implications of paired intrinsic states on the interpretation of experimental data in the s-d shell. Finally in Sec. VI we present our conclusions.

II. A SUMMARY OF HFB THEORY

A. The Quasiparticle Transformation

We assume that the nucleus can be described by a two body Hamiltonian

$$H = \sum_{\substack{ij \\ \mu\nu}} \langle i\mu | T | j\nu \rangle C_{i\mu}^\dagger C_{j\nu} + \frac{1}{4} \sum_{\substack{ijkl \\ \mu\nu\rho\delta}} \langle i\mu j\nu | V_a | k\rho l\delta \rangle C_{i\mu}^\dagger C_{j\nu}^\dagger C_{l\delta} C_{k\rho}, \quad (1)$$

where T is the kinetic energy and V is some effective two nucleon interaction. Since we choose to work in an oscillator basis, $|i\tau\rangle$ denotes a wavefunction with quantum numbers $|n_i \ell_i j_i m_i \tau\rangle$. The Hamiltonian is next transformed to one written in terms of quasiparticles

$$a_{\alpha\mu}^+ = \sum_{i\nu} [u_{\alpha\mu, i\nu} C_{i\nu}^\dagger + v_{\alpha\mu, i\nu} C_{i\nu}], \quad (2)$$

where the $u_{\alpha\mu, i\nu}$ and $v_{\alpha\mu, i\nu}$ are complex coefficients of the HFB transformation. They are determined by requiring that the quasiparticles are Fermions and that the Hamiltonian describes independent quasiparticles except for a residual interaction, i.e.:

$$H' = H - \lambda N = E'_0 + \sum_{\alpha\mu} E_{\alpha\mu} a_{\alpha\mu}^\dagger a_{\alpha\mu} + H_{INT}, \quad (3)$$

where

$$N = \sum_{i\nu} C_{i\nu}^\dagger C_{i\nu}, \quad (4)$$

is the number operator,

$$\lambda = \lambda_p |p\rangle\langle p| + \lambda_n |n\rangle\langle n|, \quad (5)$$

p and n refer to the isospin indices for the proton and neutron. λ_p and λ_n are Lagrange multipliers, and $E_{\alpha\mu}$ are the quasiparticle energies. It is H' rather than H that must be transformed for when H_{INT} is neglected the quasiparticle vacuum

$|\Phi_0\rangle$ is an eigenstate of the independent quasiparticle Hamiltonian but not of the neutron and proton number operators. The Lagrange multipliers are chosen so that

$$\langle N_p \rangle = Z \quad \langle N_n \rangle = A - Z. \quad (6)$$

The part of H' which must be transformed to give the independent quasiparticles is written

$$H'_2 = \sum_{\substack{ij \\ \mu\nu}} (\mathcal{H} - \lambda)_{i\mu, j\nu} : c_{i\mu}^\dagger c_{j\nu} : + \frac{1}{2} \sum_{\substack{ij \\ \mu\nu}} \Delta_{i\mu, j\nu} : c_{i\mu}^\dagger c_{j\nu}^\dagger : \\ + \frac{1}{2} \sum_{\substack{ij \\ \mu\nu}} \Delta_{i\mu, j\nu}^\dagger : c_{i\mu} c_{j\nu} : , \quad (7)$$

where the normal order is taken with respect to the quasiparticle vacuum and

$$\mathcal{H}_{i\mu, j\nu} = T_{i\mu, j\nu} + \Gamma_{i\mu, j\nu} \quad (8)$$

$$\Gamma_{i\mu, j\nu} = \sum_{\substack{k\ell \\ \rho\sigma}} \langle i\mu k\rho | v_a | j\nu \ell\sigma \rangle \rho_{\ell\sigma, k\rho} \quad (9)$$

$$\Delta_{i\mu, j\nu} = \frac{1}{2} \sum_{\substack{k\ell \\ \rho\sigma}} \langle i\mu j\nu | v_a | k\rho \ell\sigma \rangle t_{k\rho, \ell\sigma} . \quad (10)$$

ρ is the single particle density matrix and t is called the pairing tensor and they can be written in terms of the quasiparticle transformation

$$\rho_{i\mu, j\nu} \equiv \langle \Phi_0 | c_{j\nu}^\dagger c_{i\mu} | \Phi_0 \rangle = \sum_{\alpha\sigma} v_{\alpha\sigma, j\nu} v_{\alpha\sigma, i\mu}^* , \quad (11)$$

$$t_{i\mu, j\nu} \equiv \langle \Phi_0 | c_{j\nu} c_{i\mu} | \Phi_0 \rangle = \sum_{\alpha\sigma} u_{\alpha\sigma, j\nu} v_{\alpha\sigma, i\mu}^* . \quad (12)$$

The vacuum energy is given by

$$E_0 = E_{\text{HF}} + E_{\text{PAIR}},$$

where

$$E_{\text{HF}} = \sum_{\substack{ij \\ \mu\nu}} (T - \lambda + \frac{1}{2} \Gamma)_{i\mu, j\nu} \rho_{j\nu, i\mu} + \lambda_p Z + \lambda_n (A - Z),$$

and

$$E_{\text{PAIR}} = \frac{1}{2} \sum_{\substack{ij \\ \mu\nu}} \Delta_{i\mu, j\nu} t_{j\nu, i\mu}^\dagger. \quad (13)$$

The coefficients in the transformation (2) and the quasiparticle energies are given by the solutions of the HFB equations

$$\begin{bmatrix} (\mathcal{H} - \lambda) & \Delta \\ \Delta^\dagger & (\lambda - \tilde{\mathcal{H}}) \end{bmatrix} \begin{bmatrix} u \\ v \end{bmatrix} = E \begin{bmatrix} u \\ v \end{bmatrix}. \quad (14)$$

The matrix to be diagonalized in (14) is often referred to as the κ matrix. Since the potentials depend on the solutions to the equations, the equations must be solved by iteration until self-consistency is achieved.

B. Self-Consistent Symmetries

The HFB equations contain both the HF and BCS equations as limits. The generalized BCS equations result from choosing an initial transformation of the form

$$a_{i\mu}^\dagger = \sum_{\nu} (u_{i\mu, i\nu} c_{i\nu}^\dagger + v_{i\mu, i\nu} c_{i\nu}), \quad (15)$$

where $|\bar{i}\rangle$ is the state time conjugate to $|i\rangle$ and $|i\rangle$ is some single particle state chosen so that for any relevant set of isospin indices

$$\begin{aligned} & \langle i j | V_a | i' j \rangle \langle \langle \langle i j | V_a | i j \rangle \rangle \rangle \\ & \langle i \bar{i}' | V_a | j \bar{j} \rangle \langle \langle \langle i \bar{i} | V_a | j \bar{j} \rangle \rangle \rangle . \end{aligned} \quad (16)$$

The HFB equations may then be approximated by the usual 4×4 system of BCS equations.¹⁰ It is of course not obvious a priori that such single particle states can be found and it will be one of our important conclusions that such approximations are not valid in the s-d shell. The HF equations can be obtained by simply choosing trial wavefunctions such that all $t_{ij} = 0$. By Eq. (10) this insures $\Delta = 0$ and from the structure of Eq. (14) we see that at each stage of the iteration Δ will remain zero and finally upon convergence will give the HF solution.

This is an example of a symmetry which when initially built into the HFB equations propagates through to the final self-consistent solution. We will call these propagating symmetries (PS). It is important to consider such symmetries for a seemingly arbitrary trial wavefunction might contain one or more of them and so it may be impossible to obtain the solution with the largest binding energy from such an initial guess. Moreover the solution of a completely unrestricted HFB problem is impracticable even in the s-d shell for from Eqs. (2) and (14) we see that this would involve diagonalizing 48×48 complex matrices until self consistency is achieved. Thus it is imperative to use PS's to reduce the numerical problem. To this end we wish to specify a subset of the PS's which we will call self-consistent symmetries (SCS) and which can be uniquely defined.

It should be stressed that there are other PS's which to our knowledge can not be uniquely defined and which from time to time we have discovered numerically.

A SCS is defined as a unitary or antilinear unitary operator S which commutes with the H'_2 part of the Hamiltonian (see Eq. (7)). Sufficient conditions for such an operator to be a SCS are

- 1) The total Hamiltonian (3) is invariant under the symmetry operation, i.e.

$$[H', S] = 0 \quad (17)$$

- 2) The trial wavefunctions is invariant up to a phase under the symmetry operations, i.e.

$$S |\phi_0\rangle = e^{i\phi} |\phi_0\rangle \quad (18)$$

- 3) S maps the single particle basis states into themselves.

The proof of this theorem and a rather complete discussion of SCS's has been recently given by P. U. Sauer.¹³ If H'_2 commutes with S , then of course the quasiparticle states $a_{\alpha\mu}^+$ and $a_{\alpha'\mu'}^+ = S a_{\alpha\mu}^+ S^{-1}$ are degenerate and may be specified by the labels of the irreducible representations of the symmetry group S . Thus if we can show that our trial wavefunction satisfies conditions I, II, and III for some operator S and if the matrix Eq. (14) is reduced to block form because of this symmetry, then because we have a PS we need only diagonalize the smaller blocks effecting a large saving in effort. Moreover for discrete symmetries such as time reversal one need only solve one half the problem since the time conjugate states may be obtained from the relation

$$a_{\alpha\mu}^+ = T a_{\alpha\mu}^+ T^{-1} \quad (19)$$

For every SCS introduced the generality of the theory is reduced, but often the dynamics of the problem suggest that such symmetries will be contained in the physically relevant HF or HFB solutions,¹⁴ i.e. even if the SCS is broken in the trial wavefunction, it will be recovered at the end of the iteration process. We will now list the SCS's used in this work and briefly discuss their implications.

Parity. The quasiparticles are labeled by the parity quantum number and so the κ matrix is diagonalized separately in spaces of positive and negative parity. There can be no inversion non-invariant deformations in the intrinsic state.

Time reversal. Use of this SCS allows one to further decompose the κ matrix into blocks which define quasiparticles connected by time conjugation. In this paper we use harmonic oscillator basis states and choose our phases so that

$$T |n \ell j m \tau \rangle = (-1)^{j-m+\ell} |n \ell j - m \tau \rangle.$$

Because T acts only on the space-spin coordinates, we will suppress the isospin coordinate for the discussion of time reversal. We divide the basis states into two sets, the first containing states with $m-1/2 =$ even integer and denoted by $\{|i \rangle\}$; the second contains those states having $m-1/2 =$ odd integer. They are chosen to be the time conjugate states of the first set and denoted by $\{|\bar{i} \rangle\}$. In this paper we will restrict the pairing to be between time conjugate states, i.e., we write the transformation (2) either with $u_{\alpha,i}$ and $v_{\alpha,\bar{i}}$ or $u_{\beta,\bar{i}}$ and $v_{\beta,i}$. Making this restriction in the trial wavefunctions breaks the κ matrix into blocks and introduces a PS. However since we are dealing with even-even systems we can choose time reversal as a SCS. This implies the restriction

$$a_{\beta}^{\dagger} = a_{\bar{\alpha}}^{\dagger} = T a_{\alpha}^{\dagger} T^{-1}, \quad (20)$$

which yields the relations

$$u_{\bar{\alpha}, \bar{i}} = u_{\alpha, i}^*, \quad v_{\bar{\alpha}, i} = -v_{\alpha, \bar{i}}^*, \quad (21)$$

and finally the HFB equations reduce to

$$\begin{pmatrix} \mathcal{H} - \lambda & \Delta \\ \Delta & \lambda - \mathcal{H} \end{pmatrix} \begin{pmatrix} u \\ v \end{pmatrix} = E \begin{pmatrix} u \\ v \end{pmatrix}, \quad (22)$$

where in contrast to (14) $\mathcal{H} = (\mathcal{H})_{ij}$, $\Delta = (\Delta)_{ij}$, and both \mathcal{H} and Δ are hermitian.

Axial symmetry. This introduces a new quantum number Ω (the z-projection of angular momentum) into the specification of the quasiparticle. This symmetry is introduced by restricting the quasiparticle transformations to states $|i\rangle$ with the same value of m and states $|\bar{i}\rangle$ with $-m$. Although this symmetry is too restrictive⁵ in HF (in ^{24}Mg and ^{32}S the lowest solutions are triaxial) it is one of the main purposes of this paper to examine whether this is any longer true in HFB.

Rotational symmetry. The quasiparticles are specified by the quantum numbers jm . Such a symmetry may be introduced by restricting the transformation so that the set $\{|i\rangle\}$ have the same jm and the set $\{|\bar{i}\rangle\}$ have $j-m$. This

symmetry is in general too restrictive and in HF is valid only for doubly magic nuclei. We find within the framework of HFB that the lowest solutions in the s-d shell do not have this symmetry.

Rotations in Isospace.

Since we have a general transformation which includes the coupling of neutrons and protons there may be various SCS's in isospace. For example we might demand rotational invariance. However this would restrict us to $N = Z$ nuclei and $T = 0$ pairing. Since we limit ourselves to $N = Z$ even-even nuclei in this paper this would be a possible symmetry. However we want to examine if we can not lower the energy by allowing nonconservation of isotopic spin in the intrinsic state. One might also demand rotational invariance about the z-axis, but then we would restrict ourselves to neutron-proton pairing and we wish to allow for neutron-neutron and proton-proton pairing as well. For $N = Z$ nuclei, it is physically reasonable to expect that the ground state has the property that $\langle \tilde{T} \rangle = 0$.¹⁵ This can be ensured by choosing an operator $T' = \tau_y K$ (τ_y is two times the y component of isospin and K is the complex conjugation operator) in isospace as a SCS. With this symmetry the transformation in isospin space is written

$$\begin{pmatrix} a_1^+ \\ a_2^+ \\ \bar{a}_1 \\ \bar{a}_2 \end{pmatrix} = \begin{pmatrix} u_{1,1} & 0 & -v_{1,1} & -v_{1,2} \\ 0 & u_{1,1} & -v_{1,2}^* & v_{1,1} \\ v_{1,1} & v_{1,2} & u_{1,1} & 0 \\ v_{1,2}^* & -v_{1,1} & 0 & u_{1,1} \end{pmatrix} \begin{pmatrix} c_p^+ \\ c_n^+ \\ -c_p \\ -c_n \end{pmatrix}, \quad (23)$$

and further we choose the matrices $u_{1,1}$ and $v_{1,1}$ to be real. With this transformation the pairing potential Δ may be written

$$\Delta = \begin{pmatrix} \Delta_{pp} & \Delta_{pn} \\ \Delta_{pn}^* & -\Delta_{pp} \end{pmatrix}, \quad (24)$$

where

$$\Delta_{pn} = \Delta_{pn}^{T=1} + i \Delta_{pn}^{T=0}. \quad (25)$$

A close examination¹⁸ of Δ shows that diagonal elements of $\Delta^{T=0}$ vanish if we choose the PS that all coefficients are real, a result independent of any SCS in isospace. Consequently a complex HFB transformation is required for simultaneous $T = 0$ and $T = 1$ pairing.

In our discussion of time reversal we showed that restricting the pairing to time conjugate states gives time reversal as a SCS. This however excludes a possible mode of neutron-proton pairing where both particles are in the same space-spin state α and are coupled to $T = 0$, i.e. we could consider $\alpha\alpha$ pairing in addition to the usual $\alpha\bar{\alpha}$ pairing. Such a mode could in principle be included in the general transformation but would make the numerical calculation essentially impossible since one loses the advantage of breaking up the space into time conjugate blocks (although the solution could still have time reversal as a SCS) and further we no longer can have rotational invariance about the z-axis as a SCS. In the next section we will calculate this mode and attempt to argue numerically that it is much less coherent than the usual mode and so can be safely neglected. The lack of coherence of the $\alpha\alpha$ type of pairing can be explicitly demonstrated in the case of a simple $J = 1$ force.¹⁶

C. The Canonical Basis

In this subsection we wish to describe several approximations to the most general HFB formalism and also to describe our method for presentation of wavefunctions. This may best be done by using a theorem similar to that of Bloch and Messiah¹⁷ which states that the most general transformation B_{gen} is given by the product of three transformations:¹⁸

1) a transformation D in particle space which defines the canonical basis and is obtained by diagonalizing the density matrix; 2) a generalized BCS transformation B_{sp} ; and 3) a transformation R in the quasiparticle space.

$$B_{\text{gen}} = R B_{\text{sp}} D. \quad (26)$$

Now the well known BCS approximation consists of assuming that we know a priori the canonical basis and further that \mathcal{K} and Δ are diagonal in the space-spin part of this basis. Then the κ matrix breaks into 4×4 blocks. If there is no neutron-proton pairing the κ matrix further reduces to the familiar 2×2 matrices yielding the gap equation for the pairing of identical particles. In the HFB calculation of Ref. 11 this simplification is achieved by use of the pairing plus quadrupole Hamiltonian in which case Δ is trivially diagonal in the HF representation of the $Q \cdot Q$ force. The approximation that we used in I is to take the coupled Hartree-Bogoliubov¹⁹ and BCS equations which are equivalent to the HFB equations up to a unitary transformation and note that if the off-diagonal elements of Δ are small then they reduce to coupled generalized HF and BCS equations. Although this might intuitively seem a better approximation than BCS it still depends on Δ being diagonal in the canonical basis. In any diagonal Δ approximation R is the unit matrix. One of the major points to be explored in the present paper is the extent to which the non-zero off-diagonal elements of Δ affect the solution.

In Sec. IV we will discuss the various approximations numerically and it will be useful to express the wavefunctions in terms of the three transformations.

$$C_{r\mu}^\dagger = \sum_{iv} D_{r\mu,iv} C_{iv}^\dagger. \quad (27)$$

The isospin structure of this transformation consistent with the SCS's is

$$D = \begin{bmatrix} D_{pp} & 0 \\ 0 & D_{nn} \end{bmatrix}, \quad (28)$$

where $D_{pp} = D_{nn}$. With our choice of SCS's the second transformation B_{sp} may be written in terms of the submatrices

$$\begin{bmatrix} a_{r1}^\dagger \\ a_{r2}^\dagger \\ a_{r1}^- \\ a_{r2}^- \end{bmatrix} = \begin{bmatrix} u_{11}^r & 0 & -v_{11}^r & -v_{12}^r \\ 0 & u_{11}^r & -v_{12}^{r*} & v_{11}^r \\ v_{11}^r & v_{12}^r & u_{11}^r & 0 \\ v_{12}^{r*} & -v_{11}^r & 0 & u_{11}^r \end{bmatrix} \begin{bmatrix} C_{rp}^\dagger \\ C_{rn}^\dagger \\ C_{rp}^- \\ C_{rn}^- \end{bmatrix}, \quad (29)$$

where u_{11}^r and v_{11}^r are real numbers and v_{12}^r is complex. The third transformation is written

$$a_{\alpha\mu}^\dagger = \sum_{r\nu} R_{\alpha\mu,r\nu} a_{r\nu}^\dagger, \quad (30)$$

and the isospin structure consistent with our SCS's becomes

$$R = \begin{bmatrix} R_{11} & 0 \\ 0 & R_{22} \end{bmatrix}, \quad (31)$$

where $R_{11} = R_{22}$. The general transformation can thus be specified by giving the real orthogonal matrices D_{pp} and R_{11} , and the coefficients u_{11}^r , v_{11}^r , and v_{12}^r . It is interesting to point out that the canonical basis is doubly

degenerate and so by taking appropriate¹⁸ linear combinations of the degenerate solutions it is possible to define the pairing between two single particle states which become linear combinations of proton and neutron states with complex coefficients. These are the states which define the Bloch-Messiah canonical basis.¹⁷ We do not use this mixed neutron proton canonical basis for convenience in comparing with previous results.

III. DESCRIPTION OF THE CALCULATION

A. Method of Solution

To solve the HFB equations (14) it is important to have reliable initial guesses. In the first place using completely random guesses may introduce undesirable PS's and moreover such bad guesses may take a prohibitively long time to converge. We solve this problem in the following way:

1) We first solve the HF equations which give various HF solutions. In particular we find axially asymmetric and both prolate and oblate axially symmetric solutions, and often we find several solutions having the same shape. The HF single particle states may be written as

$$C_{\alpha\mu}^{\dagger} = \sum_i D'_{\alpha\mu, i\mu} C_{i\mu}^{\dagger} \quad (32)$$

2) We next calculate the coefficients of a generalized BCS transformation

$$\begin{bmatrix} a_{\alpha 1}^{\dagger} \\ a_{\alpha 2}^{\dagger} \\ a_{\alpha 1}^{-} \\ a_{\alpha 2}^{-} \end{bmatrix} = \begin{bmatrix} u_{\alpha} & 0 & -v_{\alpha} & -v'_{\alpha} \\ 0 & u_{\alpha} & -v'^{*}_{\alpha} & v_{\alpha} \\ v_{\alpha} & v'_{\alpha} & u_{\alpha} & 0 \\ v'^{*}_{\alpha} & -v_{\alpha} & 0 & u_{\alpha} \end{bmatrix} \begin{bmatrix} C_{\alpha p}^{\dagger} \\ C_{\alpha n}^{\dagger} \\ C_{\alpha p}^{-} \\ C_{\alpha n}^{-} \end{bmatrix} \quad (33)$$

where u_α and v_α are real and v'_α is complex. The method of solving for the u 's and v 's has been given in an earlier paper.¹⁵

3) The starting values of the HFB transformation coefficients are now given as

$$u_{\alpha\mu,iv} = D'_{\alpha\mu,iv} u_\alpha \delta_{\mu,v}$$

$$v_{\alpha 1,i1} = -v_{\alpha 2,i2} = D'_{\alpha 1,i1} v_\alpha \quad (34)$$

$$v_{\alpha 1,i2} = v_{\alpha 2,i1}^* = D'_{\alpha 1,i1} v'_\alpha$$

4) The starting value of λ is also obtained from solutions of the generalized BCS equations.¹⁵

5) With these starting values, we obtain the final solutions by iteration until self-consistency is achieved.

Once the HFB transformation has been determined we express it as a product of the three Bloch-Messiah matrices discussed in the last section. The procedure for determining them is outlined below.

1) The canonical basis is obtained by diagonalizing the density matrix (11). This gives us the transformation D of Eq. (27). ρ and t are then determined in the canonical basis.

2) We now express ρ and t in terms of the coefficients of the second transformation B_{sp} , Eq. (29). We then have the following relations

$$\rho_{pp}^r = \rho_{nn}^r = v_{11}^r{}^2 + |v_{12}^r|^2 \quad (35)$$

$$\rho_{pn}^r = \rho_{np}^r = 0 \quad (36)$$

$$t_{pp}^r = u_{11}^r v_{11}^r = -t_{nn}^r \quad (37)$$

$$t_{pn}^r = u_{11}^r v_{12}^{r*} = t_{np}^{r*}, \quad (38)$$

where $\rho_{\mu\nu}^r = \rho_{r\mu,rv}$ and $t_{\mu\nu}^r = t_{r\mu,\bar{r}v}$. u_{11}^r may be obtained from Eq. (35) as

$$|u_{11}^r| = \sqrt{1 - \rho_{pp}^r}. \quad (39)$$

We choose $u_{11}^r \geq 0$ and then v_{11}^r and v_{12}^r can be obtained from Eqs. (37) and (38).

3) Since B_{gen} , D and B_{sp} are now known R can be determined from Eq. (26). Further details can be found in Ref. 18.

B. Choice of Force

In I, we used a Rosenfeld-Yukawa force in our calculations. Since the existence and importance of the isospin pairing correlations depend on the nature of the effective interaction (for example, the relative strength of $T = 0$ vs. $T = 1$ matrix elements or the s-wave triplet to singlet strength), we have used three types of force in this work, the first two of which are commonly regarded as realistic. The rationale for using such forces in both the HF and HFB calculations is that these calculations are to be regarded as a caricature of an exact shell model calculation in a sufficiently large model space.

1. Yale t-matrix. The Yale potential²⁰ was determined by very accurate fitting of the nucleon-nucleon scattering data. Since a hard core is included, one must replace the matrix elements of V by those of t . The t-matrix

elements used in this paper are those calculated by Shakin *et al.*²¹ from the Yale potential. As is customary, the dependence of the t-matrix on the single particle wavefunctions and energies (double self-consistency) is ignored. The shell model space is confined to the lowest three oscillator shells. The oscillator parameter ($b = \sqrt{\hbar/m\omega}$) chosen is $\sqrt{3.1}$ fm. This choice of force and parameters enables us to compare our results with previous HF calculations.²²

2. Nestor-Davies-Krieger-Baranger (NDKB) potential.²³ This potential was specifically designed with no hard core for Hartree-Fock calculations. The effect of the hard core is simulated by using a velocity dependent term in the potential. In fitting the force parameters (we use set number 3), primary emphasis was given to reproducing the binding energy and equilibrium density of nuclear matter, in such a manner that the second order corrections to the binding energy are small.

3. Rosenfeld-Yukawa effective interaction. This force has been widely used in the s-d shell (see discussion in I). For the HFB calculations we truncate to the $N = 2$ oscillator shell and replace the kinetic energy by single particle energies (see I and Ref. 4). As in I we use single particle energies which correspond to the experimental ones found in ^{17}O (Rosenfeld 1) and also to energies which were used in the HF calculation²⁴ of ^{24}Mg (Rosenfeld 2). We use this force in order to compare with the results in I and for the possibility of comparing with the results of exact shell model calculations. Since the HFB method is used here in the spirit of approximating an exact shell model calculation, such a comparison should be carried out in the future.

C. Validity of Number Non-Conservation Approximations

In I we compared number non-conserving BCS with the results of exact number projection for $T = 0$ pairing. Although we found that the total energies do not change appreciably, the pairing energy was reduced by approximately 30% in the number conserving case and this was due to the drastic reduction of the dispersion of the particles across the Fermi surface (see Fig. 1 in I). For number non-conservation to be accurate we would expect that the binding energy should vary linearly with N . Because of the importance of n-p pairing this linearity will be particularly important between odd-odd and even-even $N = Z$ nuclei. A cursory glance at the experimental mass symmetries of the s-d shell even mass nuclei, shows the presence of a sharp discontinuity at the $N = Z$ even-even nuclei. For example the mass discontinuity at ^{24}Mg is $\Delta M(^{24}\text{Mg}) (= M(^{26}\text{Al}) - 2M(^{24}\text{Mg}) + M(^{22}\text{Na})) = 10.5 \text{ MeV}$. However this experimental discontinuity is of no relevance in pairing theory. Rather it will be the discontinuity calculated with the underlying HF wavefunctions. It is interesting to note that with the triaxial HF solution calculated in Ref. 22, $\Delta M(^{24}\text{Mg}) = 11.3 \text{ MeV}$. This is due to the presence of a large gap in the triaxial solution. In I it was shown that it is just this gap which prevents the (number non-conserving) pairing field from building up in the triaxial HF basis. On the other hand using the axially symmetric prolate HF solution given in Ref. 22 one gets $\Delta M(^{24}\text{Mg}) = -3.8 \text{ MeV}$. Since the mass discontinuity is relatively small in this case, a strong number non-conserving $T = 0$ pair field builds up on this solution (see Sec. IV and I). However this discontinuity is large enough to

severely limit the accuracy of the number non-conserving BCS method. To our knowledge a number conserving HFB calculation has not been carried out. We do not attempt to do so in this paper, however one can get a rough estimate of the validity of the number non-conserving method by calculating the discontinuity for the canonical basis. Using the canonical basis functions given in Sec. IV we find $\Delta M(^{24}\text{Mg}) = -3.7$ MeV, $\Delta M(^{32}\text{S}) = -7.1$ MeV, and $\Delta M(^{36}\text{Ar}) = 5.0$ MeV. This suggests that the number non-conserving method is not any more valid in HFB than in BCS.

D. The Absence of α - α and $T = 1$ Pairing

In Sec. II it was pointed out that we have not included the possibility of $\alpha\alpha$ pairing in our calculations but in I it has already been shown that a dominance of a pair field of one kind precludes the build up of other pairing fields. For example $T = 1$ pairing is suppressed by the $T = 0$ field for all $N = Z$ even even nuclei. This remains true for the solutions presented in this paper. With the Yale force and a space of three oscillator shells we also investigated $\alpha\alpha$ pairing and find ^{24}Mg has a binding energy of -130.53 MeV, while ^{32}S and ^{36}Ar have binding energies of -225.12 MeV and -291.07 MeV respectively. These solutions are obtained with the nuclei artificially constrained to be axially symmetric. When this constraint is removed the nuclei either gain ~ 0.3 MeV in binding energy or fall into the triaxial HF solutions. For pure $\alpha\bar{\alpha}$ pairing the binding energies for these nuclei are -132.53 MeV, -229.66 MeV, and -291.76 MeV. The relative lack of coherence of the $\alpha\alpha$ pair field is clear. It is therefore expected that this field will be suppressed by the stronger $\alpha\bar{\alpha}$ pair field in a more general calculation although this has not yet been investigated numerically.

IV. NUMERICAL RESULTS

A. Comparison of the HF and Canonical Basis and the Validity of the Approximation used in I.

In Table I we give the HFB wavefunctions for the solutions with the largest binding energy in terms of the three Bloch-Messiah transformations defined in Eqs. (26) - (31). These wavefunctions were obtained with the Yale t-matrix with three oscillator shells.

As pointed out in Sec. II, a measure of the deviation of our previous approximation from the complete HFB is given by the deviation of R from the unit matrix. It can be seen from Table I, that this deviation although appreciable for ^{24}Mg and ^{32}S , is very large for ^{36}Ar . A similar measure can be obtained by comparing the HF wavefunctions D' given in Ref. 21 with the canonical wavefunctions D of Table V. Again large deviations are due to the fact that Δ is not diagonal in the canonical basis. In Table II we give the matrix Δ in the canonical basis for ^{24}Mg , ^{32}S , and ^{36}Ar . Not surprisingly we find that Δ has a large off diagonal elements for all three nuclei. Although ^{24}Mg has large off diagonal elements, the canonical basis is remarkably similar to the HF solution and the dispersions calculated from the HFB and the diagonal Δ approximation of I are also very similar. Thus for this particular case only the third transformation is effected by the non diagonal elements of Δ . We know of no criteria that will tell a priori whether Δ will be diagonal in the canonical basis so we therefore conclude that in the s-d shell the complete HFB is necessary since the diagonal Δ approximation may be misleading. This is especially true for excited state calculations which depend on the quasiparticle energies and wavefunctions.

In Table III we compare E_{HF} , E_{PAIR} , and E_{TOTAL} for the HF + BCS approximation,¹⁰ the diagonal Δ HFB approximation of I , and the complete HFB of this paper. From this comparison we may conclude that HFB always gives the largest binding energy. Second, we observe that the pairing energy increases in the HFB (largely at the expense of HF energy) often by more than a factor of two. This is understandable because the HF wavefunctions were derived to maximize the HF

binding energy. When the pairing field is allowed to build up simultaneously and self-consistently, it should be expected that the pair field will gain energy at the expense of the HF field.

B. Physical Properties of the HFB Solutions

In Table IV, we list certain properties which describe the intrinsic states for all the paired HFB solutions we have obtained for all the $N = Z$ even even s - d shell nuclei with all the forces we have discussed in Sec. III. The NDKB1 solutions were obtained in a space of three oscillator shells using the Nestor-Davies-Krieger-Baranger force. The NDKB2 solutions were obtained using the same force but in a space expanded to include four oscillator shells. The parameters characterizing the HFB intrinsic states that we shall discuss are defined below. We specify the shape of an intrinsic state by giving their quadrupole and hexadecapole moments

$$Q_{20} = \left\langle \sum_{i=1}^A r_i^2 Y_{20}(\Omega_i) \right\rangle$$

$$Q_{40} = \left\langle \sum_{i=1}^A r_i^4 Y_{40}(\Omega_i) \right\rangle . \quad (40)$$

It is also usual to define the shape of a nucleus with the size independent shape parameters β_2 and β_4 which for axially symmetric deformations are defined by

$$\beta_2 = \frac{4\pi}{5} \frac{Q_{20}}{R_2^2 A} \quad (41)$$

$$\beta_4 = \frac{4\pi}{7} \frac{Q_{40}}{R_4^4 A} , \quad (42)$$

where R_2 is taken to be the root mean square radius

$$R_2 = \frac{1}{A} \left\langle \sum_{i=1}^A r_i^2 \right\rangle, \quad (43)$$

and

$$R_4 = \frac{1}{A} \left\langle \sum_{i=1}^A r_i^4 \right\rangle, \quad (44)$$

and A is the mass number. From Table IV we make the following conclusion. HFB theory is less ambiguous than HF + BCS in the sense that as many as four different HF + BCS solutions converge to the same HFB solution. All of the forces lead to more or less the same conclusions about the physical properties of intrinsic states. Also we observe that the energy gaps are on the average 20% larger in the HFB solutions compared with the HF + BCS approximation indicating an increased stability for these solutions. Finally we observe that increasing the shell space to include the next major shell has the expected property that deformation increases due to core polarization, reflected by a substantial increase in β_2 of approximately 40%.

Also from Table IV one can see there is a definite tendency for the increase of pairing energy as one expands the shell model space. The amount of increase is only 20% at ^{24}Mg but increases to 90% at ^{36}Ar . The effective energy gap of two quasiparticle excitations displayed in the last column of Table IV increases from 20% in ^{24}Mg to 45% in the case of ^{36}Ar due to the enlargement of the space. This demonstrates that the solutions become more stable as one enlarges the shell model space.

The effect of various factors on the underlying self-consistent field such as the truncations of the shell space or the inclusion of pairing

correlations can be demonstrated in a pictorial manner by plotting the mass distribution defined by

$$\mu(\underline{r}) = \sum_{ij} \sum_{k=1}^A \langle i | \delta(\underline{r} - \underline{r}_k) | j \rangle \rho_{ji} \quad (45)$$

Figures 1-6 present the equidensity contours of various HF and HFB solutions. All of these plots show the projection of the density distribution on a plane which has the axis of symmetry as the vertical axis. The densities are normalized with respect to the corresponding maximum density taken arbitrarily as unity.

In Fig. 1 we plot the contours of constant density for paired ^{32}S calculated with a space including only three oscillator shells. A similar plot but now including four oscillator shells is given in Fig. 2. Apart from the conspicuous increase in the overall deformation, a comparison of the two figures reveals that the enhancement of pairing correlations is associated with a considerable shift of mass towards the center of the nucleus. The effect of pairing correlations on the nuclear shape and in particular the tendency toward higher symmetry due to pairing is demonstrated with Figs. 3 and 4 by comparing the density distribution of the prolate HF solution and the prolate HFB solution for ^{24}Mg . In this case it can also be seen that there is an alpha particle clustering in the HF solution and that this effect is reduced in the HFB solution. A similar comparison is given for ^{36}Ar in Figs. 5 and 6 where we plot the density distributions for the oblate HF and HFB solutions respectively. Here again a big reduction in deformation due to pairing is clearly demonstrated. It will be shown later that this reduction is responsible for correcting the discrepancy in the HF description for ^{36}Ar .

The changes in shape of the HFB intrinsic states are also reflected in the total angular momentum contained in each state. It is interesting to compare the values of $\langle J^2 \rangle$ calculated with the wavefunctions given in Table I and the solutions with largest binding energy which are quoted in Ref. 22. When the values of $\langle J^2 \rangle$ are expressed in units of \hbar^2 a comparison shows ^{24}Mg (22.4 vs. 24.4), ^{32}S (19.5 vs. 25.4), and ^{36}Ar (13.0 vs. 16.5) where the value from the HFB calculation appears first. The decrease in angular momentum for the ^{24}Mg and ^{32}S HFB intrinsic states is because the HF solutions are triaxial and such non-symmetric shapes contain large amounts of angular momentum.

Before we conclude this section we would like to mention that the inertial parameter $A (= \frac{\hbar^2}{2\mathcal{I}}$ where \mathcal{I} is the moment of inertia) is calculated using the Inglis cranking model.²⁵ The expression for the moment of inertia for an HFB intrinsic state is

$$\mathcal{I} = 2 \sum_{\substack{i\mu \\ k\nu \\ \sigma}} \frac{\langle i\mu | j_x | j\mu \rangle \langle k\nu | j_x | l\nu \rangle}{E_\sigma - E_0} v_{\alpha\rho, i\mu}^* u_{\alpha\rho, k\nu}^* v_{\beta\tau, l\nu}^* u_{\beta\tau, j\mu} \quad (46)$$

In this expression E_0 is the vacuum energy and E is the energy of a two quasiparticle state ($E_\sigma = E_0 + E_{\alpha\rho} + E_{\beta\tau}$) and where the sum on σ is made in such a way as to avoid double counting the two quasiparticle states. One might expect on observing the structure of (46) that since the gaps increase in HFB over the values obtained from the HF + BCS approximation that the inertial parameters will be somewhat larger. The limitations of the cranking model have been discussed in I.

V. COMPARISON WITH EXPERIMENT

It was pointed out in Sec. III that the HFB solutions with the largest binding energy exhibit only $T = 0$ pairing. This was also a feature of the calculations in I and the reasons for this phenomena are discussed there. Another general feature of the HFB solutions is the near degeneracy [in $\langle H \rangle$] of several solutions. These solutions have a large overlap and so only one of them is physically relevant as far as the low energy spectrum is concerned. Self-consistent field calculations are usually unable to make the proper choice among these nearly degenerate solutions because of the neglect of many higher order corrections (see discussion in I). Nevertheless it is often possible to compare properties predicted by the various intrinsic states with experimental information and so eliminate the non-physical states. Below we will consider the nuclei individually.

^{20}Ne . The ground intrinsic state is adequately described by a prolate HF solution.²⁶ For this solution pairing corrections are small²⁷ and can not be calculated by our methods (see discussion in I).

^{24}Mg . For ^{24}Mg HF theory predicts²⁸ the ground state shape to be triaxial (in agreement with SU_3 theory²⁹). In I we discussed in detail several pieces of experimental evidence which show that this nucleus is best described by an axial prolate intrinsic state.^{30,31} Since then an exact projection of angular momentum has been carried out³² which shows that this intrinsic state does not produce an $I(I+1)$ spectrum for either the $K = 0$ or $K = 2$ bands which feature is in sharp contradiction to experiment. Further the $K = 0$ and $K = 2$ band splitting is underestimated by 1.7 MeV. With Yale-Shakin t -matrix elements, the HFB equations give almost degenerate solutions: 1) the triaxial HF state with $\langle H \rangle = -133.14$ MeV, 2) a prolate paired state with $\langle H \rangle = -132.53$ MeV, and

3) an oblate paired state where $\langle H \rangle = -132.05$ MeV. From the discussion in the last paragraph we rule out the HF solution as a suitable intrinsic state. Recently, the quadrupole moment of the first $2+$ state of ^{24}Mg has been measured³³ and is found to have a negative sign consistent with a prolate shape for the intrinsic state. This rules out the axial oblate solution. The axially symmetric prolate solution seems to be consistent with experimental data. It trivially gives the $I(I+1)$ spectra for the $K = 0$ and $K = 2$ bands. The cranking value of the inertial parameter for the ground band is found to be 0.33 MeV, and the unperturbed position of the lowest $K = 2+$ two quasiparticle state is 4.81 MeV. The paired prolate intrinsic state gives a much more consistent description of experimental data than any HF state.

²⁸Si. It is well known that HF predicts two nearly degenerate and orthogonal solutions, one being axially symmetric prolate and the other oblate. The ordering of the two states, based on the value of $\langle H \rangle$, depends on the particular force used.^{22,34} Experimentally one does not see two low-lying $K = 0$ bands and it has been theoretically shown that the bands can not be separated by mixing.³⁵ Furthermore recent experimental measurements³⁶ of the quadrupole moment of the first $2+$ state show that the band is in fact oblate. But the ground state band deviates considerably from an $I(I+1)$ spectrum since the $J = 0$ member of the band is too low. It has recently been suggested³⁷ that this depression could be explained by the interaction of the $J = 0$ member with a coexisting spherical state. However HF calculations with realistic forces predict a spherical state that is much too high to be associated with the coexisting spherical state seen at 4.98 MeV. Unfortunately the solutions to the HFB equations also give force dependent results. The Yale t -matrix gives identical

results to HF because both the prolate and oblate HF solutions have too large single particle gaps to permit pairing correlations using our methods. However with the NDKB potential, we find an isospin paired axially symmetric prolate solution almost degenerate with the prolate and oblate HF solutions. This HFB prolate solution has a significant overlap with both the HF solutions since all the single particle states are partially occupied because of the pairing correlations. With this potential one can discard the prolate HF solution because of its small energy gap and the prolate HFB solution because of its large overlap with the oblate HF solution. The latter solution appears to be in essential agreement with experiment if the coexistence picture is accepted. However we are unable to produce a low energy spherical solution with any of the potentials used.

^{32}S . HF theory predicts a triaxial intrinsic shape for ^{32}S . This state is very peculiar having the inertial parameters about all three axes equal and a vanishing quadrupole distortion parameter.⁷ Physical predictions made from such an intrinsic state do not agree with experiment. However it is possible to interpret the experimental data using an axially symmetric intrinsic state if one allows for the coexistence³⁷ of a spherical intrinsic state which appears at 3.78 MeV. The solutions to the HFB equations again give three solutions with similar binding energies. With the Yale t-matrix we find the triaxial HF solution with $\langle H \rangle = -227.74$ MeV, a paired axially symmetric oblate state with $\langle H \rangle = -229.66$ MeV, and a paired axially symmetric prolate state with $\langle H \rangle = -224.53$ MeV. All three solutions have significant overlap and only one can be an acceptable intrinsic state. The asymmetric-state can be eliminated from the experimental data. However since there has been no experimental measure

of the quadrupole moment of the first $2+$ state, we can not choose between the oblate and prolate axially symmetric solutions. As in the case of ^{28}Si we were not able to find a spherical solution with a sufficiently low energy to be the coexisting state.

^{36}Ar . This nucleus is very interesting because phenomenologically one can interpret the low lying spectrum as being vibrational. On the other hand, HF calculations give a deformed oblate state ($\langle H \rangle = -291.07$ MeV for the Yale t -matrix) with a large energy gap and a small value of the inertial parameter. This intrinsic state of course predicts low lying rotational structure in disagreement with experiment. The solutions to the HFB equations offer a possible answer to the problem. One obtains a paired oblate solution lower in energy than the HF solution ($\langle H \rangle = -291.77$ MeV). This HFB solution is remarkable in that its inertial parameter is unusually large ($A = 0.62$). This means that the rotational states appear at energies comparable with the two quasiparticle states with the result that rotational structure will be destroyed.

A recent paper by de Swiniarski et al.³⁸ has used a coupled channel analysis of inelastic scattering data to determine the β_2 and β_4 values for the $N = Z$ even-even nuclei. In Fig. 7 we compare our calculated values with the results of their analysis. The theoretical numbers are calculated with the wavefunctions in Table II for ^{24}Mg , ^{32}S , and ^{36}Ar . We use the wavefunctions from Ref. 21 for ^{20}Ne and ^{28}Si . In Fig. 8 we compare the inertial parameters calculated with these wavefunctions with the values obtained from experiment as discussed in I. We also plot the HF results. A comparison of Fig. 2 in I and Fig. 8 show that the inertial parameter increases in HFB over the HF + BCS approximation by 20%. As pointed out in Sec. IV, this is understood by the increase in the gap.

VI. CONCLUSION

In previous works we have investigated the existence of generalized isospin ($T = 0$ and $T = 1$) pairing with the assumption that the pair potential is diagonal in space-spin co-ordinates. The HFB equations have now been solved without making this approximation and also using "realistic force." All approximations to the HFB equations (HF and BCS, iterating between HF and BCS and HB + BCS) have serious defects. They fail to approximate the exact (HFB) wavefunctions. The first two approximations underestimate the pairing energy (often by a factor of 2 or 3). The HFB canonical single particle basis often bears no similarity to the HF single particle basis.

The third transformation of the Bloch-Messiah theorem may not be approximated by the unit matrix, nor is the pair potential diagonal in the canonical basis.

Iterating between the HF and the BCS equations in an attempt to permit both degrees of freedom to interact with one another¹ is an even worse approximation to HFB than merely solving the BCS equations with the trivial HF basis but allowing HF single particle energies to be modified by pairing. Presumably this results from the lack of self-consistency in the former method. To permit both $T = 0$ and $T = 1$ pairing it is necessary to use complex quasiparticle co-ordinates. In practice, however, $T = 0$ pairing always suppresses $T = 1$ pairing.

Nevertheless the results regarding the equilibrium shapes remain much the same as in I: $T = 0$ pairing restores axial symmetry to ^{24}Mg and ^{32}S and provides an explanation for the nonexistence of low-lying rotational states in ^{36}Ar . We finally conclude that isospin ($T = 0$) pairing is an important correlation effect for light nuclei. As far as we know, this is the only occasion

that pairing occurs in nature in other than singlet S states. Furthermore, the isospin pairing phenomenon is distinguished by the largeness of the pairing energy. Much work, theoretical and experimental, remains to be done before a complete understanding of this phenomenon of isospin pairing is achieved.

ACKNOWLEDGMENTS

The authors wish to thank Dr. P. Sauer, Dr. S. N. Tewari, and Mr. H. Wolter for useful discussion. They particularly wish to thank Mr. Wolter for help in calculating the inertial parameters. The authors also wish to acknowledge the help of Mr. P. S. Rajasekhar in calculating two body matrix elements. One of us (J.B.) wishes to thank Dr. N. K. Glendenning and the Division of Nuclear Chemistry of the Lawrence Radiation Laboratory for their kind hospitality during the summer of 1969.

FOOTNOTES AND REFERENCES

- * Work performed under the auspices of the U. S. Atomic Energy Commission.
1. D. L. Hill and J. A. Wheeler, Phys. Rev. 89, 1106 (1953).
 2. See for example, Bohr and Mottelson, book to be published.
 3. S. G. Nilsson, Kgl. Danske Videnskab. Selskab. Met. Fys. Medd. 29, No. 16 (1955).
 4. G. Ripka in Lectures in Theoretical Physics, Univ. of Colorado, 1965.
 5. G. Ripka, in Advances in Nuclear Physics (1967).
 6. J. Bar-Touv, A. Goswami, A. L. Goodman and G. L. Struble, Phys. Rev. 178, 1670 (1969).
 7. M. K. Benerjee, C. A. Levinson and G. J. Stephenson, Jr., Phys. Rev. 178, 1709 (1969).
 8. L. Satpathy, D. Goss and M. K. Banerjee, Phys. Rev. 183, 887 (1969).
 9. P. Sauer, A. Faessler and H. Wolter, Nuclear Physics A125, 257 (1969).
 10. A. L. Goodman, G. L. Struble and A. Goswami, Phys. Letters 26, B260 (1968).
 11. M. Baranger and K. Kumar, Nucl. Phys. A92, 608 (1967).
 12. C. Bloch, Lecture notes, Tata Institute, Bombay, 1962, unpublished.
 13. P. U. Sauer, Nuovo Cim. 57B, 62 (1968).
 14. See for example, Refs. 7 and 8.
 15. H. T. Chen and A. Goswami, Phys. Letters 24, B257 (1967).
 16. A. Goswami and L. S. Kisslinger, Phys. Rev. 140, B26 (1965).
 17. C. Bloch and A. Messiah, Nucl. Phys. 39, 95 (1962).
 18. A. L. Goodman, Thesis, 1969, University of California, Lawrence Radiation Laboratory Report UCRL-19514, unpublished.
 19. K. Dietrich, H. T. Mang, and J. Pradhan, Z. für Physik 190, 357 (1966).

20. K. E. Lassila, M. H. Hall, Jr., H. M. Ruppel, F. A. McDonald and G. Breit, Phys. Rev. 128, 881 (1962).
21. C. M. Shakin, Y. R. Waghmare and M. H. Hull, Phys. Rev. 161, 1006 (1967).
22. M. K. Pal and A. P. Stamp, Phys. Rev. 158, 924 (1967).
23. Nestor, Davis, Krieger and Baranger, Nucl. Phys. A113, 14 (1968).
24. J. Bar-Touv and I. Kelson, Phys. Rev. 138, B1035 (1965).
25. D. R. Inglis, Phys. Rev. 96, 1059 (1954); Ibid. 97, 1701 (1955).
26. S. N. Tewari, Phys. Letters 29B, 5 (1969).
27. M. K. Pal and A. P. Stamp, Nucl. Phys. A99, 228 (1967).
28. First pointed out in Ref. 24.
29. For the most recent SU_3 based shell model calculation see Arima et al., Nucl. Phys. A138, 273 (1969).
30. J. C. Parikh, Phys. Letters 26, B607 (1968).
31. B. Cujec, Phys. Rev. 136, B1305 (1969); G. J. McCallum and B. J. Schwerby, Phys. Letters 25, B109 (1967).
32. B. Giraud and P. U. Sauer, Proceedings of the International Nuclear Physics Conference, Montreal, Canada, 1969.
33. O. Hausser, T. K. Alexander, D. Pelte, and B. W. Hooton, and H. C. Evans, Phys. Rev. Letters 22, 359 (1969).
34. S. Dasupta and M. Harvey, Nucl. Phys. A94, 602 (1967).
35. S. N. Tewari and D. Grillot, Phys. Rev. 177, 1717 (1969).
36. O. Hausser, T. K. Alexander, D. Pelte, and B. W. Hooton, and H. C. Evans, Phys. Rev. Letters 23, 320 (1969).
37. J. Bar-Touv and A. Goswami, Phys. Letters 28, B391 (1968).
38. R. de Swiniarski, C. Glashauser, D. L. Hendrie, J. Sherman, A. D. Bacher, and E. A. McClatchie, Phys. Rev. Letters 23, 317 (1969).

TABLE CAPTIONS

Table I. HFB wavefunctions for the lowest energy nontrivial HFB solutions for ^{24}Mg , ^{32}S and ^{36}Ar . Calculations are done with the Yale-Shakin potential in the s-p-s-d shell basis. $\Omega\pi$ denotes the component of total angular momentum on the symmetry axis and the parity respectively for each orbital. E denotes the quasiparticle energies in MeV. The general quasiparticle transformation is displayed as a product of three transformations as explained in the text. In the column giving $[\text{Im } v_{12}]^2$, (the sign of $\text{Im } v_{12}$) is given in the parenthesis. Note that $v_{11} = \text{Re } v_{12} = 0$ for all the solutions. λ is the Fermi energy.

Table II. The $T = 0$ pair potential (in MeV) in the canonical basis, corresponding to the solutions in Table I.

Table III. A comparison of pairing theories. E_{HF} , E_{PAIR} and E_{TOTAL} denote the Hartree-Fock, pairing, and the total energies in MeV.

Table IV. Paired HFB solution in the s-d shell. Only non-trivial solutions are displayed. In the third column denoting the shape of the HFB solution, the shape of the trial HF wavefunction is also shown in parenthesis: P: prolate, O: oblate, S: spherical. In case there is more than one HF solution of a given shape, they are distinguished by an additional member e.g., P1, P2, etc. The numbers in the gap column are the sum of the two smallest quasiparticle energies.

Table I. HFB Wavefunctions.

$\Omega\pi$	E	Transformation R				$[\text{Im}v_{12}]^2$	Transformation D						
		^{24}Mg											
							<u>$1d_{5/2}$</u>						
5/2+	3.777				1.000	(+)0.034	1.000						
							<u>$1d_{5/2}$</u>	<u>$1d_{3/2}$</u>					
-3/2+	2.651				0.167	0.986	(+)0.008	0.347	-0.938				
	7.982				0.986	-0.167	(-)0.684	0.938	0.347				
							<u>$1s_{1/2}$</u>	<u>$1d_{5/2}$</u>	<u>$2s_{1/2}$</u>	<u>$1d_{3/2}$</u>			
1/2+	2.158				0.247	0.923	-0.296	0.015	(+)0.014	0.143	-0.409	-0.747	0.504
	5.058				0.926	-0.134	0.351	-0.036	(-)0.317	0.024	-0.617	-0.175	-0.767
	6.503				0.285	-0.361	-0.888	0.021	(+)0.953	0.067	0.672	-0.622	-0.396
	49.655				0.024	-0.011	0.036	-0.999	(+)1.000	0.987	0.029	0.155	-0.027
										<u>$1p_{3/2}$</u>			
-3/2-	19.334					1.000	(-)0.997			1.000			
										<u>$1p_{3/2}$</u>	<u>$1p_{1/2}$</u>		
1/2-	16.958					0.990	0.139	(-)0.996		0.570	0.821		
	26.094					-0.139	0.990	(+)0.998		0.821	-0.570		

$\lambda = -9.150 \text{ MeV}$

(continued)

Table I. continued

$\Omega\pi$	E	Transformation R				$[\text{Im}v_{12}]^2$	Transformation D			
^{32}S										
							<u>$1d_{5/2}$</u>			
5/2+	7.073				1.000	(-)0.981	1.000			
							<u>$1d_{5/2}$ $1d_{3/2}$</u>			
-3/2+	2.931				0.906	0.422	(+)0.527	0.712	0.702	
	5.337				0.422	-0.906	(-)0.949	0.702	-0.712	
							<u>$1s_{1/2}$ $1d_{5/2}$ $2s_{1/2}$ $1d_{3/2}$</u>			
1/2+	3.238	0.322	0.937	-0.136	0.011	(-)0.107	0.106	0.487	-0.533	-0.684
	5.425	0.378	-0.260	-0.884	0.086	(+)0.480	0.039	0.643	-0.306	0.702
	6.468	0.868	-0.235	0.435	-0.052	(-)0.974	0.158	-0.591	-0.765	0.199
	55.521	0.010	-0.000	0.100	0.995	(-)0.999	0.981	0.017	0.193	0.014
							<u>$1p_{3/2}$</u>			
-3/2-	29.564				1.000	(+)0.997	1.000			
							<u>$1p_{3/2}$ $1p_{1/2}$</u>			
1/2-	21.848				0.998	0.068	(-)0.991	0.734	-0.680	
	28.358				0.068	-0.998	(+)0.996	0.680	0.734	

$$\lambda = -14.245 \text{ MeV}$$

(continued)

Table I. continued

$\Omega\pi$	E	Transformation R				$[\text{Im}v_{12}]^2$	Transformation D			
^{36}Ar										
5/2+	8.012	1.000				(-)0.993	<u>1d_{5/2}</u>			
-3/2+	2.488	0.830	0.557			(+)0.877	<u>1d_{5/2}</u>	<u>1d_{3/2}</u>		
	6.771	0.557	-0.830			(-)0.980	0.703	0.711		
1/2+	2.750	0.608	0.754	-0.249	0.003	(-)0.322	<u>1s_{1/2}</u>	<u>1d_{5/2}</u>	<u>2s_{1/2}</u>	<u>1d_{3/2}</u>
	4.927	0.793	-0.561	0.239	-0.022	(+)0.852	0.088	0.451	-0.528	-0.715
	6.486	-0.041	0.343	0.938	-0.038	(-)0.988	0.042	0.635	-0.368	0.678
	57.983	0.014	-0.002	0.042	0.999	(-)0.999	0.105	-0.627	-0.752	0.173
-3/2-	31.500	1.000				(+)0.998	<u>1p_{3/2}</u>			
1/2-	26.044	0.964	0.267			(-)0.994	<u>1p_{3/2}</u>	<u>1p_{1/2}</u>		
	30.354	0.267	-0.964			(+)0.998	0.741	-0.671		
$\lambda = -16.772 \text{ MeV}$										

Table II. $T = 0$ Pair Potential in the Canonical Basis

$\Omega\pi$	^{24}Mg				^{32}S				^{36}Ar			
5/2+	1.372				-1.934				-1.372			
-3/2+	1.428	0.678			3.355	0.466			2.508	0.425		
	0.678	-2.604			0.466	-2.166			0.425	-1.526		
1/2+	1.189	0.378	-0.116	1.058	-3.707	-0.365	-0.530	-0.402	-3.862	-0.553	-0.264	-0.610
	0.378	-2.589	0.845	-0.458	-0.365	3.561	-0.103	0.019	-0.553	2.755	-0.256	0.039
	-0.116	0.845	2.547	0.367	-0.530	-0.103	-1.940	-0.989	-0.264	-0.256	-1.360	-0.310
	1.058	-0.458	0.367	1.656	-0.402	0.019	-0.989	-4.104	-0.610	0.039	-0.310	-4.016
-3/2-	-2.178				3.411				2.620			
1/2-	-2.264	-0.022			-4.153	-0.015			-4.003	-0.034		
	-0.022	2.537			-0.015	3.524			-0.034	2.707		

Table III. A comparison of Pairing Theories.

Method	E_{HF}	E_{PAIR}	E_{TOTAL}
^{24}Mg			
HF + BCS	-126.02	-6.31	-132.33
Approx. HFB	-126.53	-5.58	-132.11
HFB	-124.73	-7.80	-132.53
^{32}S			
HF + BCS	-219.01	-4.75	-223.76
Approx. HFB	-218.94	-4.88	-223.83
HFB	-215.32	-9.21	-224.53
^{36}Ar			
HF + BCS	-283.71	-3.39	-287.10
Approx. HFB	-282.76	-3.92	-286.68
HFB	-282.24	-9.52	-291.76

Table IV. Paired HFB Solutions in the s-d Shell

Nucleus	Force	Shape	Mode	E_{PAIR}	E_{TOTAL}	Q_{20}	Q_{40}	Gap
^{20}Ne	Rosenfeld 2	Oblate (0)	T = 0	-7.625	-41.697	-5.9	25.9	4.78
		Prolate (P2)	T = 0	-6.587	-41.444	2.7	-53.5	4.76
	Yale	Prolate (S)	T = 0	-2.324	-101.505	15.4	80.0	4.74
^{24}Mg	Rosenfeld 1	Prolate (P2)	T = 0	-6.438	-77.526	15.6	-14.9	5.68
		Oblate (01,02)	T = 0	-6.551	-77.238	-13.0	40.8	5.44
	Rosenfeld 2	Prolate (P1)	T = 0	-4.576	-95.170	15.6	-0.5	5.20
		Oblate (01,02,03)	T = 0	-6.858	-93.865	-12.4	58.1	4.80
	Yale	Prolate (P)	T = 0	-7.802	-132.527	19.0	-12.1	4.32
		Oblate (01,02)	T = 0	-17.205	-132.049	-12.1	31.4	5.98
NDKB 1	Prolate (P)	T = 0	-8.121	-110.388	15.9	13.4	4.98	
		T = 0	-11.802	-109.301	-12.5	47.5	4.22	
NDKB 2	Prolate (P)	T = 0	-9.637	-116.651	22.5	6.0	5.76	
		T = 0	-15.887	-114.131	-16.6	52.8	5.28	
^{28}Si	Rosenfeld 1	Prolate (02)	T = 0	-7.234	-123.420	0.13	116.0	4.70
		Oblate (02)	T = 0	-2.207	-150.041	-0.5	-96.5	5.72
	Rosenfeld 2	Prolate (03)	T = 0	-6.050	-147.808	0.14	110.5	3.80

(continued)

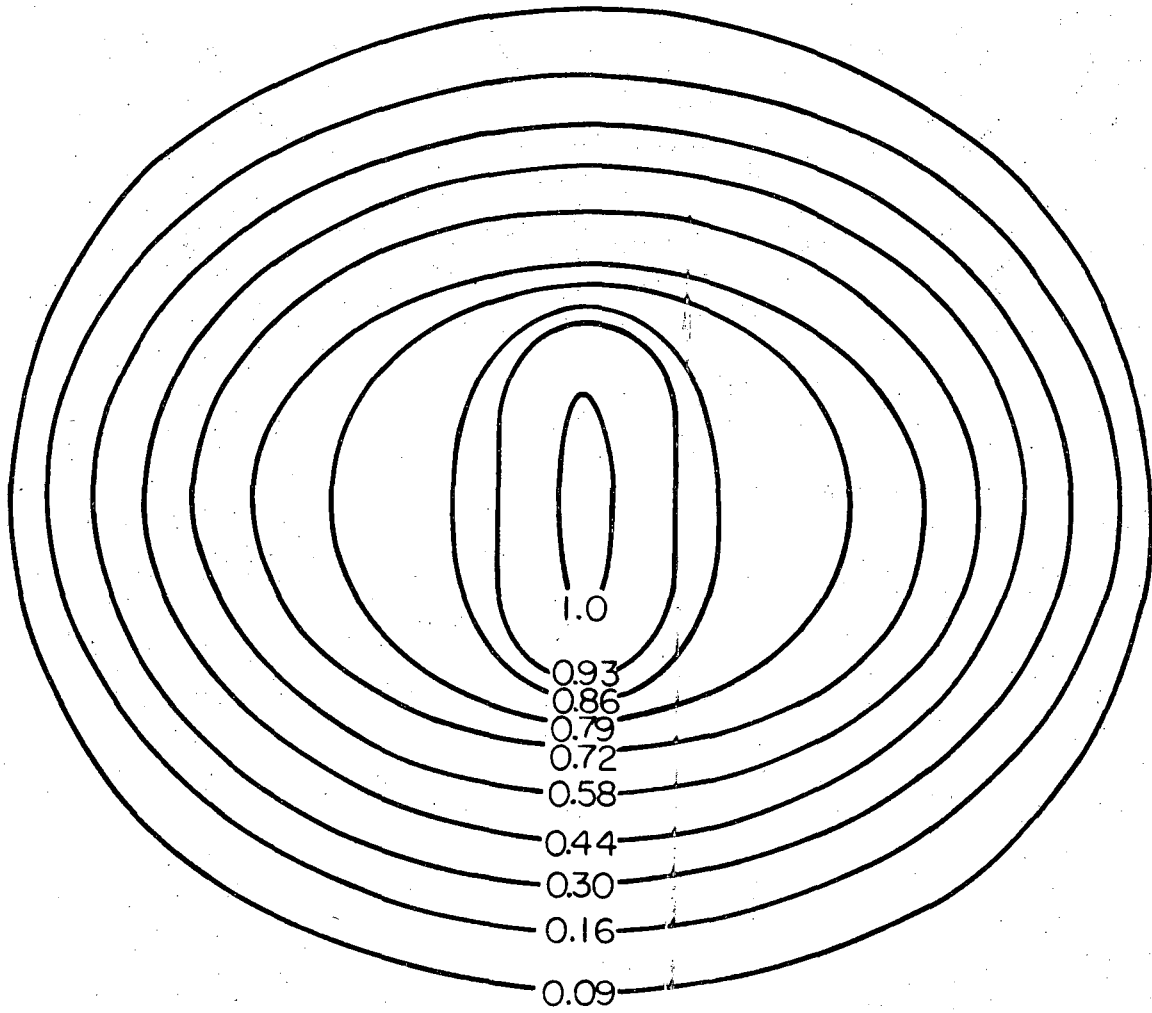
Table IV. continued

Nucleus	Force	Shape	Mode	E_{PAIR}	E_{TOTAL}	Q_{20}	Q_{40}	Gap
^{32}S	NDKB 1	Prolate (P,S)	T = 0	-9.933	-140.610	15.1	-20.9	3.76
		Prolate (02)	T = 0	-14.375	-138.733	3.1	-84.0	3.72
	NDKB 2	Prolate (02,S)	T = 0	-8.359	-146.853	24.9	-72.0	4.40
	Rosenfeld 1	Oblate (02,03)	T = 0	-5.835	-178.385	-1.3	-110.0	5.62
		Prolate (P)	T = 0	-7.276	-178.179	6.5	-94.5	5.76
		Prolate (S)	T = 0	-12.724	-176.173	3.4	37.9	4.74
	Rosenfeld 2	Oblate (01,03)	T = 0	-1.385	-212.901	-1.5	-95.8	5.30
	Yale	Oblate (NDKB1-0)	T = 0	-13.233	-229.658	-17.0	2.5	5.86
		Prolate (P)	T = 0	-9.208	-224.531	13.6	-66.3	4.58
		NDKB 1	Oblate (0)	T = 0	-6.988	-179.696	-15.5	5.9
		Prolate (P,S)	T = 0	-6.031	-179.266	12.8	-38.2	3.94
^{36}Ar	NDKB 2	Oblate (0)	T = 0	-9.977	-183.910	-20.4	0.9	4.14
		Prolate (P,S)	T = 0	-10.953	-183.153	16.8	-52.6	5.94
	Rosenfeld 1	Prolate (P,S)	T = 0	-7.722	-237.234	4.9	-26.3	4.36
	Rosenfeld 2	Prolate (P,S)	T = 0	-5.079	-277.826	3.9	-21.5	3.74
	Yale	Oblate (P,S)	T = 0	-9.523	-291.765	-11.3	-37.0	4.58
	NDKB 1	Prolate (P,S)	T = 0	-5.904	-224.664	6.0	-17.7	2.72
	NDKB 2	Prolate (P)	T = 0	-11.260	-226.519	7.5	-19.9	3.94

FIGURE CAPTIONS

- Fig. 1. Constant density contour plot for the oblate HFB solution of ^{32}S within the space of s-p-s-d oscillator orbitals. The calculations were done for the NDKB or Rms radius = 2.877 fm. The densities are given in units of 0.276 fm^{-3} .
- Fig. 2. Constant density contour plot for the oblate HFB solution of ^{32}S within the space of s-p-s-d-p-f orbitals again using the NDKB face. Rms radius = 2.870 fm. The densities are given in units of 0.296 fm^{-3} .
- Fig. 3. Constant density contour plot for the prolate HF solution of ^{24}Mg obtained with the Yale-potential. Rms radius = 2.853 fm. The densities are given in units of 0.240 fm^{-3} .
- Fig. 4. Constant density contour plot for the prolate HFB solution of ^{24}Mg obtained with the Yale potential. Rms radius = 2.856 fm. The densities are given in units of 0.246 fm^{-3} .
- Fig. 5. Constant density contour plot for the lowest oblate HF solution of ^{36}Ar obtained with the Yale force. Rms radius = 3.017 fm. The densities are given in units of 0.302 fm^{-3} .
- Fig. 6. Constant density contour plot for the oblate HFB solution of ^{36}Ar obtained with the Yale potential. Rms radius = 3.018 fm. The densities are given in units of 0.300 fm^{-3} .
- Fig. 7. The calculated values of distortion parameters β_2 and β_4 are compared with the experimental values of de S'viniarski et al.³⁸ For ^{20}Ne and ^{28}Si the theoretical value corresponds to the HF value.
- Fig. 8. The theoretical value of the moment of inertia parameter $\hbar^2/2\mathcal{I}$ (in MeV) are compared with the experimental values. For ^{28}Si and ^{32}S , the experimental values given are as extracted in Ref. 37. For ^{20}Ne and ^{28}Si the HFB value corresponds to the HF value.

^{32}S
NDKB HFB
Six orbitals



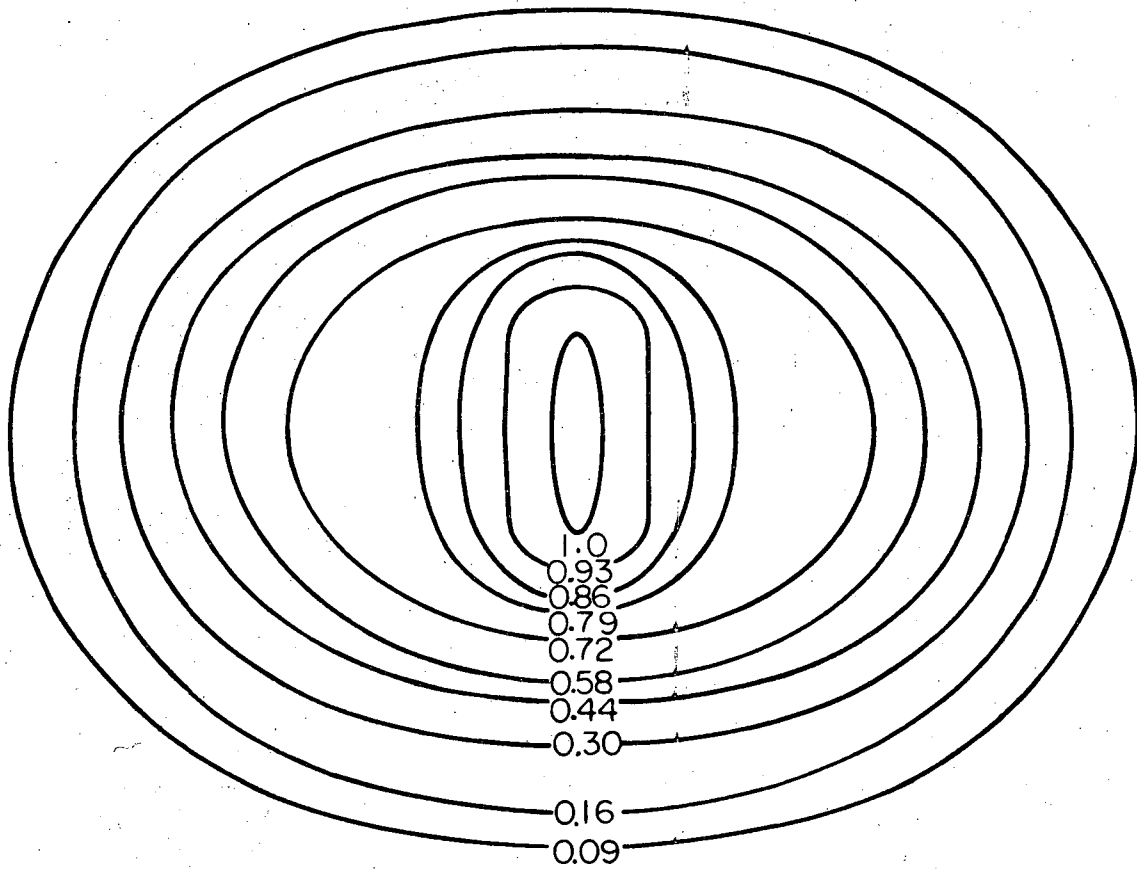
XBL 6912 - 6350

Fig. 1

^{32}S

NDKB HFB

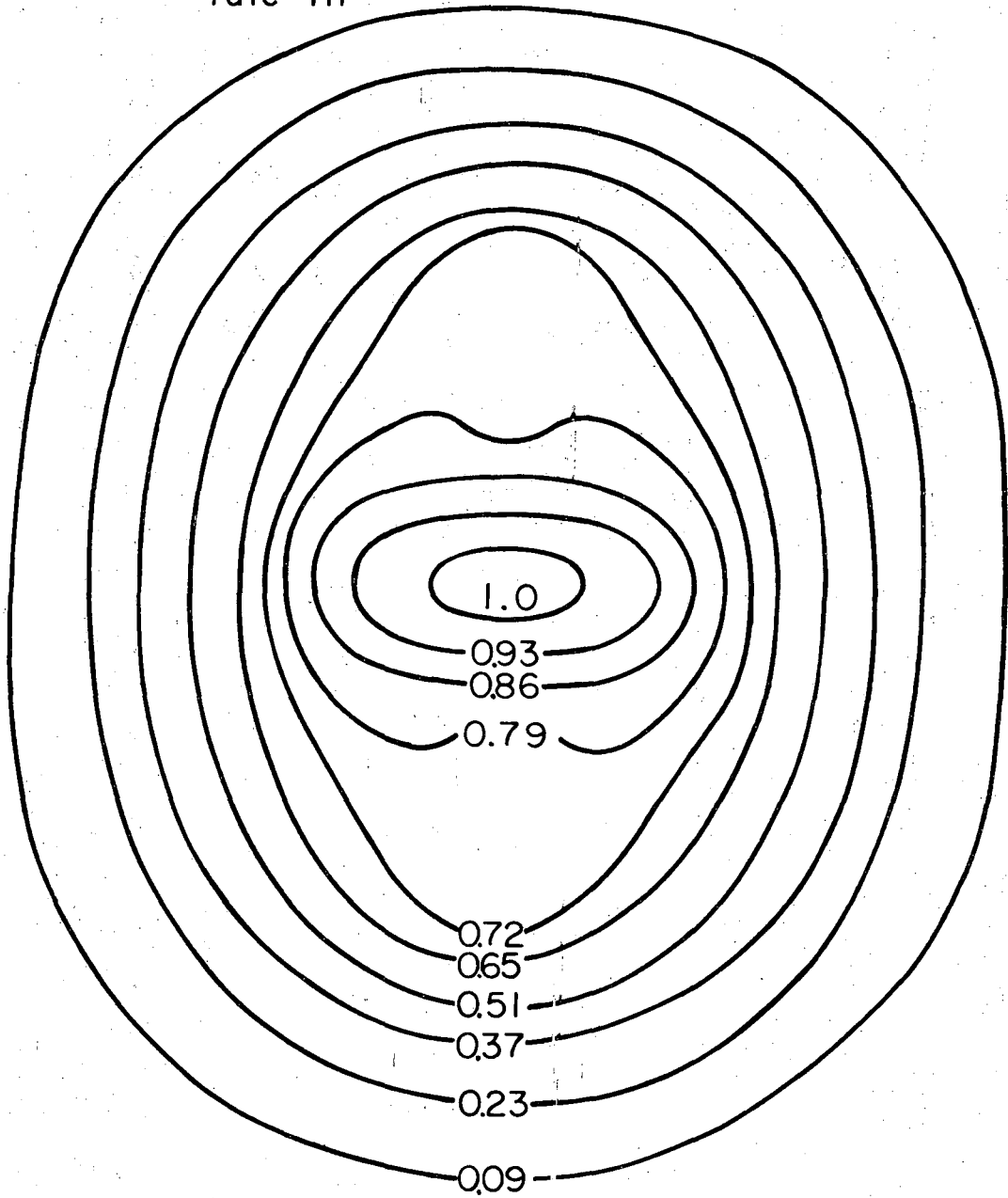
10 orbitals



XBL6912 - 6346

Fig. 2

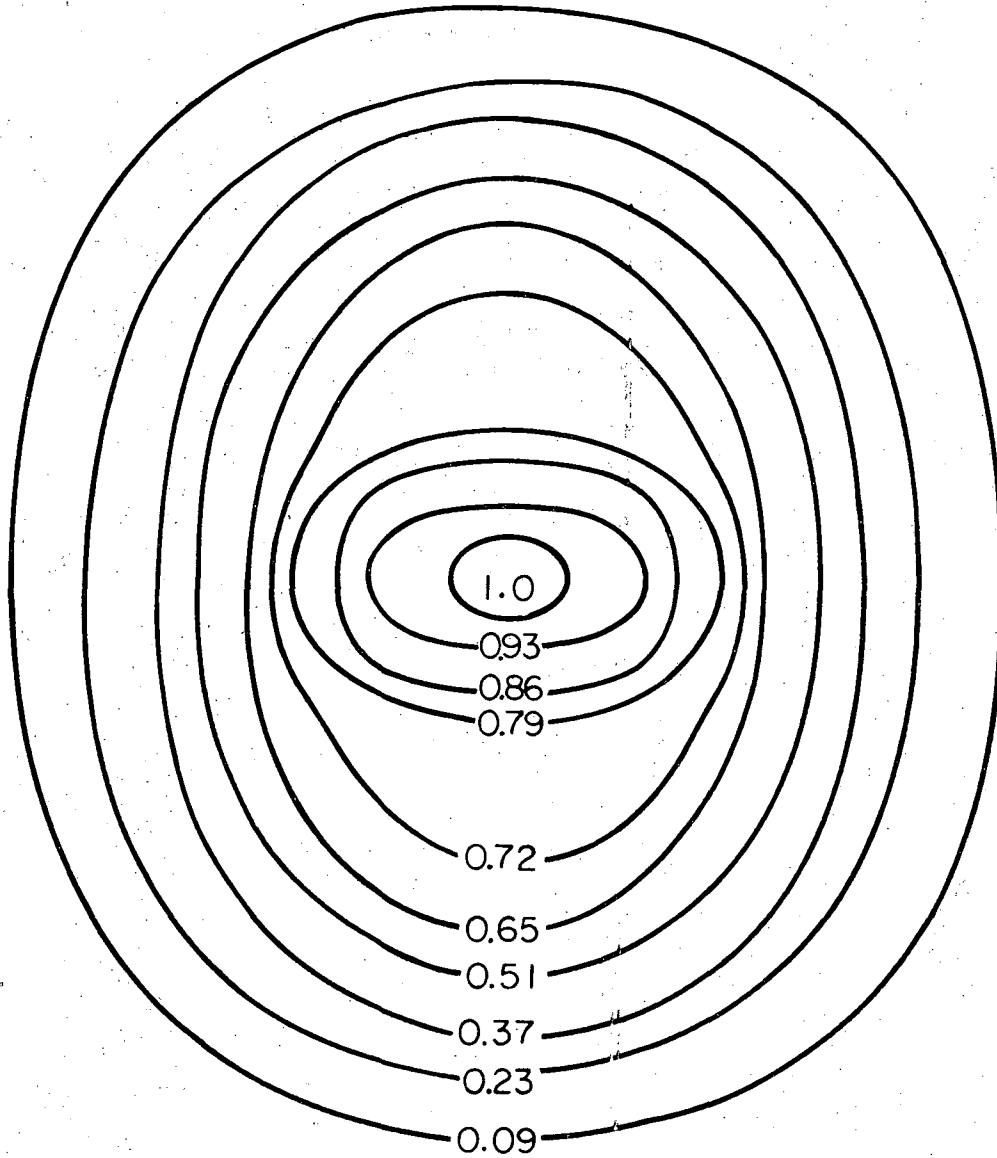
^{24}Mg
Yale HF



XBL 6912 - 6345

Fig. 3

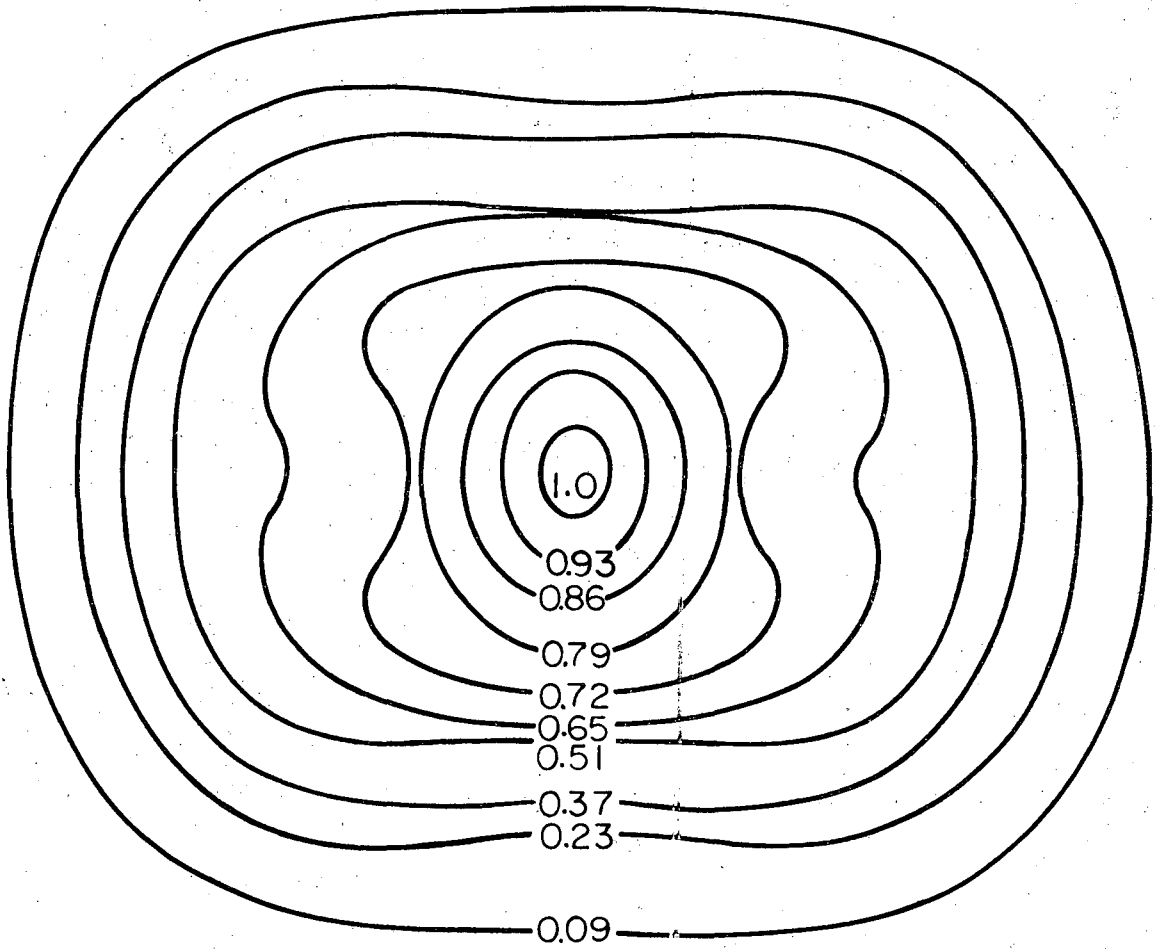
^{24}Mg
Yale HFB



XBL6912 - 6349

Fig. 4

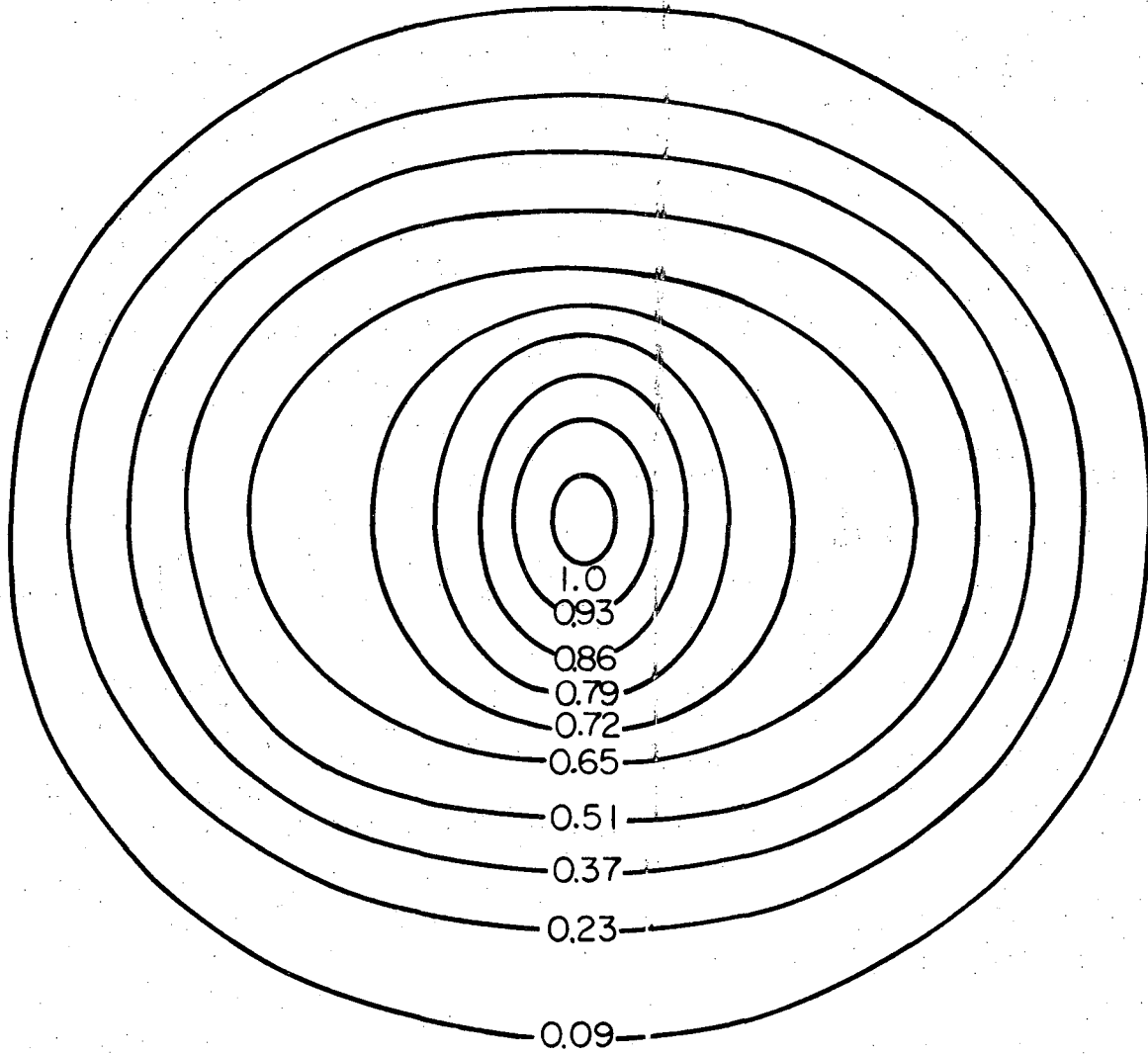
^{36}Ar
Yale HF



XBL 6912 - 6351

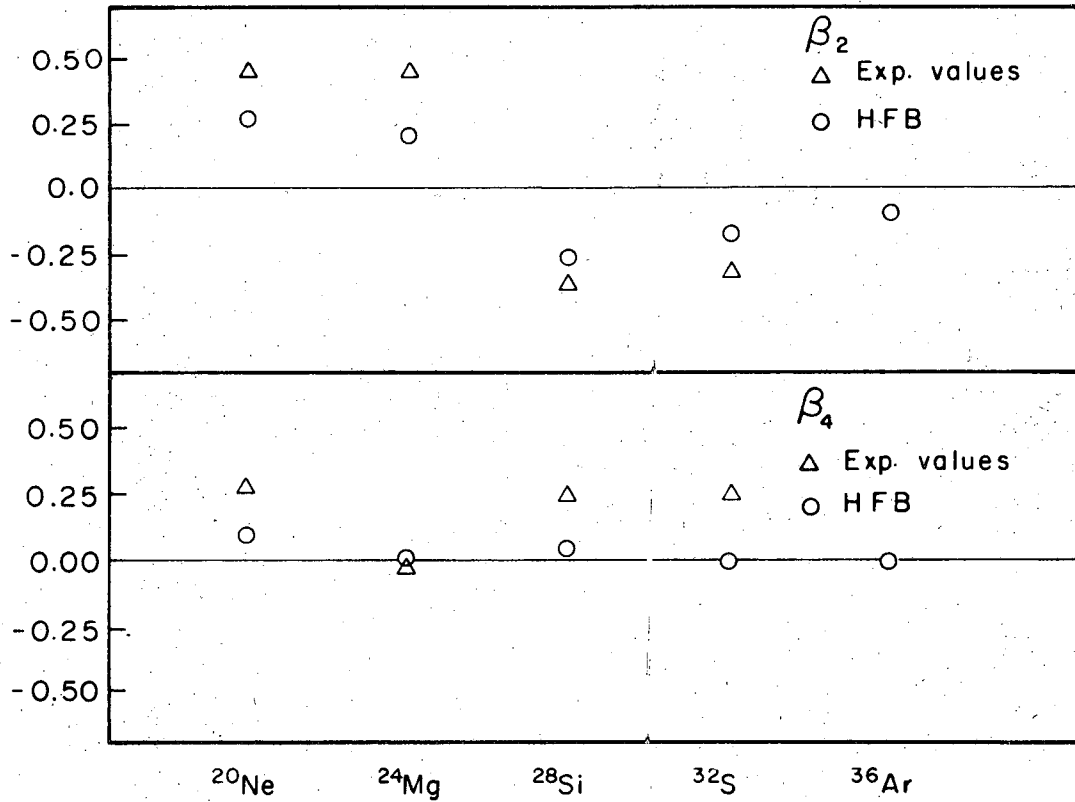
Fig. 5

^{36}Ar
Yale HFB



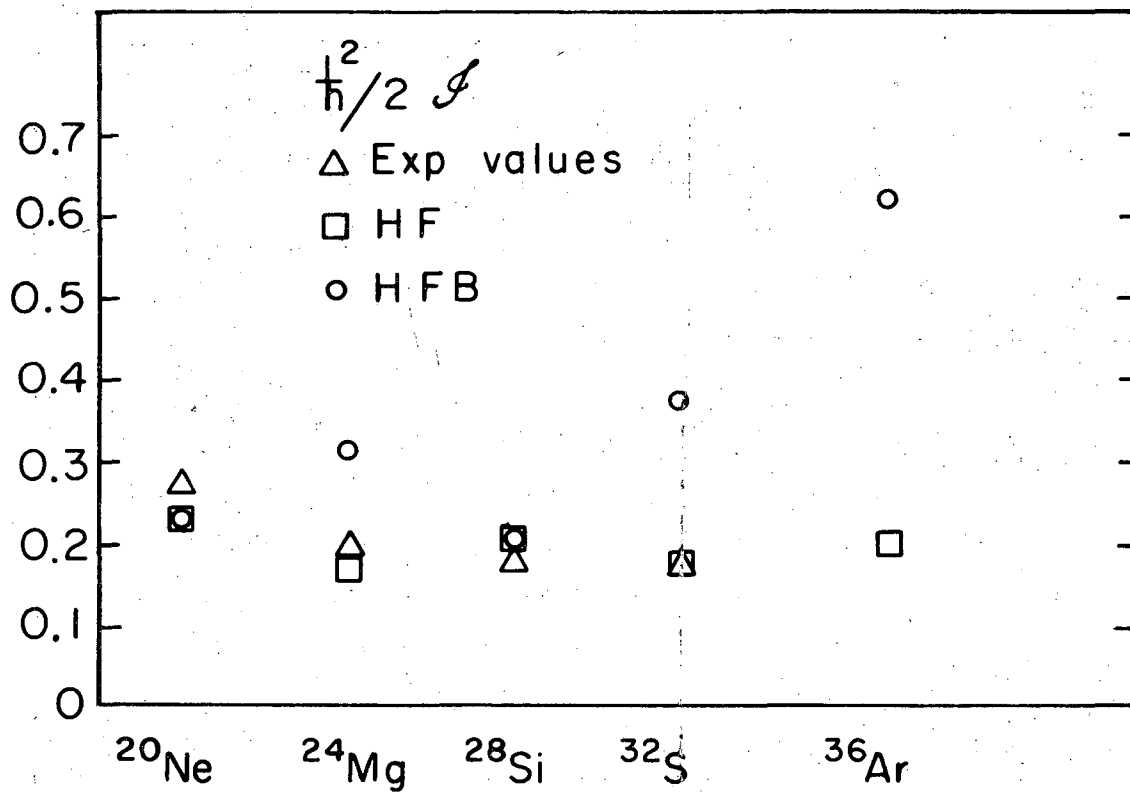
XBL6912-6347

Fig. 6



XBL6912-6352

Fig. 7



XBL 6912-6343

Fig. 8

LEGAL NOTICE

This report was prepared as an account of Government sponsored work. Neither the United States, nor the Commission, nor any person acting on behalf of the Commission:

- A. Makes any warranty or representation, expressed or implied, with respect to the accuracy, completeness, or usefulness of the information contained in this report, or that the use of any information, apparatus, method, or process disclosed in this report may not infringe privately owned rights; or*
- B. Assumes any liabilities with respect to the use of, or for damages resulting from the use of any information, apparatus, method, or process disclosed in this report.*

As used in the above, "person acting on behalf of the Commission" includes any employee or contractor of the Commission, or employee of such contractor, to the extent that such employee or contractor of the Commission, or employee of such contractor prepares, disseminates, or provides access to, any information pursuant to his employment or contract with the Commission, or his employment with such contractor.

TECHNICAL INFORMATION DIVISION
LAWRENCE RADIATION LABORATORY
UNIVERSITY OF CALIFORNIA
BERKELEY, CALIFORNIA 94720